NACA TN 3994

NATIONAL ADVISORY COMMITTEE FOR AERONAUTICS

TECHNICAL NOTE 3994

STATIC STRENGTH OF CROSS-GRAIN 7075-T6 ALUMINUM-ALLOY EXTRUDED BAR CONTAINING FATIGUE CRACKS

By Walter Illg and Arthur J. McEvily, Jr.

Langley Aeronautical Laboratory
Langley Field, Va.

Washington
April 1957

NATIONAL ADVISORY COMMITTEE FOR AERONAUTICS

TECHNICAL NOTE 3994

STATIC STRENGTH OF CROSS-GRAIN 7075-T6 ALUMINUM-ALLOY EXTRUDED BAR CONTAINING FATIGUE CRACKS

By Walter Illg and Arthur J. McEvily, Jr.

SUMMARY

Cross-grain specimens made of 7075-T6 aluminum-alloy extrusion were subjected to repeated axial loads until fatigue cracks of various lengths were formed. The specimens were then subjected to static tests to determine the residual static strength. Small cracks resulted in disproportionately large reductions of static strength. Comparison of these results with results previously obtained for loading in the with-grain direction revealed no significant difference. However, it is cautioned that cases may arise in which the cross-grain residual static strength of 7075-T6 or other materials is considerably inferior to the with-grain residual static strength, depending upon the relative shapes of the stress-strain curves. The effects of biaxiality and ductility on the notch sensitivity under static loading of sharply notched specimens are discussed in appendixes.

INTRODUCTION

The repeated stresses to which modern aircraft structures are subjected make the initiation and growth of fatigue cracks likely during the service life of the aircraft. In order to design a fail-safe structure which takes into account the likelihood of these fatigue cracks, a knowledge of the remaining static strength of parts containing cracks of various lengths is necessary. Toward this end, a large number of tests have been performed (ref. 1) to determine the static strength of aluminum-alloy specimens containing transverse fatigue cracks with the load applied parallel to the grain.

In addition to loading parallel to the grain, loading in the cross-grain direction may, of course, arise in many actual situations. This cross-grain loading may cause the formation of fatigue cracks running parallel to the grain, and since properties in the cross-grain direction have a reputation for being in general inferior to those in the with-grain direction, there is concern that the static strength of such cracked parts might be extremely low. A review of available literature on cross-grain properties of aluminum alloys revealed that the grain

direction has little effect on the fatigue properties (ref. 2). However, no data were found on the effect of grain direction on the static strength of aluminum alloys containing fatigue cracks.

The purpose of this paper is to present some data pertinent to this problem. The material investigated was 7075-T6 extruded bar stock, tested in the cross-grain direction. The results are compared with those predicted by a method of static-strength analysis developed in reference 1. The effects of biaxiality and ductility on the static strength of parts containing stress raisers are discussed.

SYMBOLS

A_o	minimum cross-sectional area of specimen without fatigue cracks or saw cuts, sq in.
E	Young's modulus, ksi
E_n	secant modulus for nominal stress on net section, ksi
E_u	secant modulus corresponding to point of maximum stress on stress-strain curve, ksi
K_N	Neuber "engineering" stress concentration factor
K_u	stress concentration factor for ultimate tensile strength
S	nominal stress on net section, ksi
S_o	maximum load divided by A_o, ksi
S_u	ultimate tensile strength of material, ksi
ρ_e	effective radius of curvature, in.
ρ_u	Neuber material constant for ultimate tensile strength, in.
σ	stress required for plastic flow
$\sigma_1, \sigma_2, \sigma_3$	principal stresses, $\sigma_1 > \sigma_2 > \sigma_3$

EXPERIMENTS

Material

The specimens for this investigation were machined from four extruded bars of 7075-T6 aluminum alloy, each with a cross section of 3/4 inch by 6 inches. The with-grain static-strength properties of this material have been investigated previously and are reported on in reference 1. The cross-grain and with-grain mechanical properties, based on tests of 1/2-inch round tensile specimens taken from the central portion of the bar stock, are given in table I. Complete stress-strain curves representative of both directions were obtained with a dial-gage extensometer and are presented in figure 1.

Specimens

Since the length in the cross-grain direction was limited to 6 inches, a specimen, shown in figure 2, was designed with serrated grip surfaces in order to obtain a reasonable length of test section. These serrations, which were made with a tool that had a point ground to a 0.02-inch radius, meshed with similar surfaces in the grip proper. It was necessary to cut relief grooves with 3/16-inch radius near the first serrations to prevent fatigue failures there.

The curved edges of the reduced section of the specimens were machined with a milling cutter that had a $1\frac{3}{8}$-inch radius. The theoretical stress concentration factor for the 1/4-inch central hole was 2.5.

Fourteen cross-grain specimens were tested. In addition, three specimens of the same configuration but with the grain direction parallel to the axis of the specimens were tested. Results for these three specimens were compared with the results for more standard specimens reported in reference 1 in order to evaluate the effect of shape of specimen on the static strength.

Tests and Testing Procedure

All testing was done in a 120-kip-capacity testing machine (ref. 3) which is shown in figure 3. An exploded view of the grips is given in figure 4. The tendency of the free ends of the jaws to diverge under load was overcome by the application of pressure clamps over each jaw. A photograph of a specimen in place is presented in figure 5 with the

pressure clamps omitted for clarity. In order to minimize bending stresses due to misalinement of the test specimens in the grips, a special order of assembly was followed. First, the serrated jaws and end plates of the grip system were bolted to the specimen apart from the testing machine. This unit was then fixed to the upper head of the machine and the lower end was bolted to the lower head.

The cyclic loads were applied automatically and were controlled by an elongation limit switch attached to the lower grip of the machine. Fatigue cracks were initiated by repeatedly applying tension loads so that the stresses on the net section varied between 55 ksi and approximately 5 ksi. The speed of testing was about 45 cycles per minute during the initial stages. After a few thousand cycles the surface of the central hole was checked with a penetrant dye to facilitate the detection of small fatigue cracks. As soon as a crack was discovered, the load was reduced in an effort to prevent specimen failure during the period of crack propagation. The cyclic loads were monitored with an electrical load-measuring device that utilizes strain gages on the grip.

In most cases, when a crack had reached a predetermined size the specimen was statically tested to failure and the maximum load was noted. In a few cases, in spite of precautions taken, the specimens failed during cyclic loading. For these, the failing load was taken to be the maximum cyclic load applied at the time of failure. After fracture the areas of the fatigue-cracked surfaces were measured with a planimeter.

Results

In this investigation the static strength of a cracked specimen is defined in terms of the material strength as determined by standard tensile tests. The results for the cross-grain specimens are presented in figure 6 as a plot of the percentage of material tensile strength remaining (based on the original net cross-sectional area) against the percentage of the original area that was cracked. A dashed line is used to represent the strength that the specimens would have if the percentage loss of strength were equal to the percentage loss of area.

In most cases the fatigue cracks originated at the root of the notch near the middle of the thickness and progressed in a plane perpendicular to the loading direction. Usually, multiple cracks were formed, and whenever the test was sufficiently long they joined to form a single crack front. The fracture surfaces of the cross-grain specimens lay more nearly in a plane than did those of the three with-grain specimens.

For purposes of comparison, figure 7 presents the results for the with-grain and cross-grain specimens of 7075-T6 of the present investigation and also the results for the with-grain specimens of 7075-T6 and

2024-T4 aluminum alloy previously reported in reference 1. The curves in figure 7 were calculated by using the method for predicting the strength of cracked specimens outlined in reference 1. In making the calculations, both the effective radius of curvature of a fatigue crack ρ_e and the Neuber material constant for ultimate tensile strength ρ_u were taken to be 0.0036 inch, as in reference 1.

The results of the investigation are also given in table II.

DISCUSSION

The results of the tests reveal that for both the with-grain and cross-grain directions the static strength is considerably reduced by a fatigue crack, the most disproportionate loss occurring for a small crack. The data also indicate that the residual static strength is essentially the same in both directions for this lot of 3/4- by 6-inch 7075-T6 extrusions. Since the results for the three with-grain specimens are generally in line with the results of reference 1, it is concluded that the special shape of the specimens in the present investigation had little effect on the static strength.

A comparison of the experimental data and the theoretical curves (fig. 7) shows that a rather large and unconservative discrepancy exists for both with-grain and cross-grain 3/4-inch-thick specimens made of 7075-T6 extruded bar. In contrast, a similar comparison between theory and experiment for sheet specimens (0.1-inch-thick) generally showed good agreement (ref. 1). The discrepancy for thick specimens is discussed in appendix A, and the conclusion is reached that it is due to the effects of biaxiality on the flow and fracture characteristics of thick specimens. When these effects are included in the analysis, an improvement between theory and experiment is obtained, as shown in figure 8. (For convenience, the same value of E_u has been taken for both the with-grain and cross-grain 7075-T6 extrusions, and therefore the theoretical curve is the same for both.) Thus far only 0.1-inch-thick and 3/4-inch-thick specimens have been investigated. Experimental work on other thicknesses is necessary to elucidate more fully the effect of thickness on the static strength of cracked parts.

One of the aims of this investigation was to determine whether the cross-grain residual static strength is inferior to the with-grain. The results indicate that for the 3/4- by 6-inch extrusion there is little difference between the two. However, no generalization should be made on the basis of the present results for, as shown in appendix B, cases may arise wherein the cross-grain residual static strength is

considerably inferior to the with-grain. The essential factors in determining relative behavior are the stress-strain curves in the directions of interest.

Figure 1 shows that for the 3/4-inch-thick 7075-T6 extrusion the two stress-strain curves are similar and the analysis (ref. 1) predicts that the residual static strength should also be similar, a prediction which is borne out in the present investigation. In contrast, figure 9 shows synthesized stress-strain curves for a 7075-T6 extrusion, $1\frac{1}{4}$ by by $4\frac{1}{2}$ inches, based on data presented in reference 2. Here it is seen that the stress-strain curves in the plastic region differ markedly. Predicted curves of residual static strength plotted against cracked area, with the effects of biaxiality neglected, are shown in figure 10. The cross-grain residual static-strength properties are predicted to be considerably inferior to the with-grain properties for this material.

Also pertinent to the present investigation is a consideration of the effect of the shape of the stress-strain curve and the effect of ductility in general on the notch sensitivity under static loading of materials. These factors are discussed in appendix B, where it is shown that an elongation of at least 6 percent is necessary to insure sufficient ductility to reduce the elastic stress concentration factors associated with sharp notches such as fatigue cracks to a relatively low level.

CONCLUSIONS

The static strength in the cross-grain direction of 3/4- by 6-inch 7075-T6 extrusions is considerably reduced by the presence of a fatigue crack. This reduction in strength is about the same in the cross-grain as in the with-grain direction. However, theoretical predictions indicate that this similarity in behavior is not necessarily general, but depends upon the relative shapes of the stress-strain curves for the directions of interest.

Langley Aeronautical Laboratory,
National Advisory Committee for Aeronautics,
Langley Field, Va., January 29, 1957.

APPENDIX A

EFFECT OF BIAXIALITY ON STATIC STRENGTH OF NOTCHED FLAT SPECIMENS

As can be seen from figure 7, rather large and unconservative discrepancies exist between experiment and theory, for both with-grain and cross-grain 3/4-inch-thick specimens. On the other hand, the comparisons of reference 1 indicated that predictions by the same method for sheet specimens were generally good. One possible reason for this behavior is that the material properties vary through the thickness of the specimen, but, since the cracks originated in the middle of the thickness and the material stress-strain curves utilized in the analysis were taken from the same region, this factor should be relatively unimportant. A more important reason for the discrepancy is that the effects of biaxiality have been neglected.

Biaxial effects arise from the tendency of the material to contract in the thickness direction as the stress at the tip of the crack is increased. In thin specimens there is little restraint to this motion and hence biaxial effects are negligible; therefore, good agreement is found between theory and experimental results for thin specimens. However, as the thickness of the specimen increases, there is a corresponding increase in resistance to lateral contraction because of the restraint of the surrounding material, which has less tendency to contract than does the material at the tip of the crack where stresses are concentrated. Under such circumstances, a tensile stress is developed in the thickness direction which varies from zero at the surface to a maximum at midthickness. The result is a stress state at the tip of the crack at midthickness characterized by a high tensile stress in the loading direction, a much smaller tensile stress, depending upon the thickness, in the thickness direction, and zero stress in a direction perpendicular to the other two directions.

At present there is no quantitative theory for the computation of this biaxial stress state in the plastic range or of its effect on static strength. However, a semiempirical approach can be utilized for improved predictions of static strength of thick parts containing fatigue cracks. Such an approach requires consideration of the effect of biaxiality on both the flow and fracture characteristics of the material.

The work of Taylor and Quinney (ref. 4) and others has established that the octahedral shear-stress yield criterion well describes the

results of combined stress tests on aluminum. According to this theory, plastic flow occurs when the state of stress in principal-stress space lies outside an ellipsoid whose equation is

$$(\sigma_1 - \sigma_3)^2 + (\sigma_2 - \sigma_1)^2 + (\sigma_3 - \sigma_2)^2 = 2\sigma^2$$

where σ_1, σ_2, and σ_3 are the principal stresses and σ is the flow stress in simple tension.

At the tip of a fatigue crack, $\sigma_3 = 0$ and therefore

$$\sigma_1^2 - \sigma_2\sigma_1 + \sigma_2^2 = \sigma^2$$

This equation may be represented by an ellipse as shown in the following sketch:

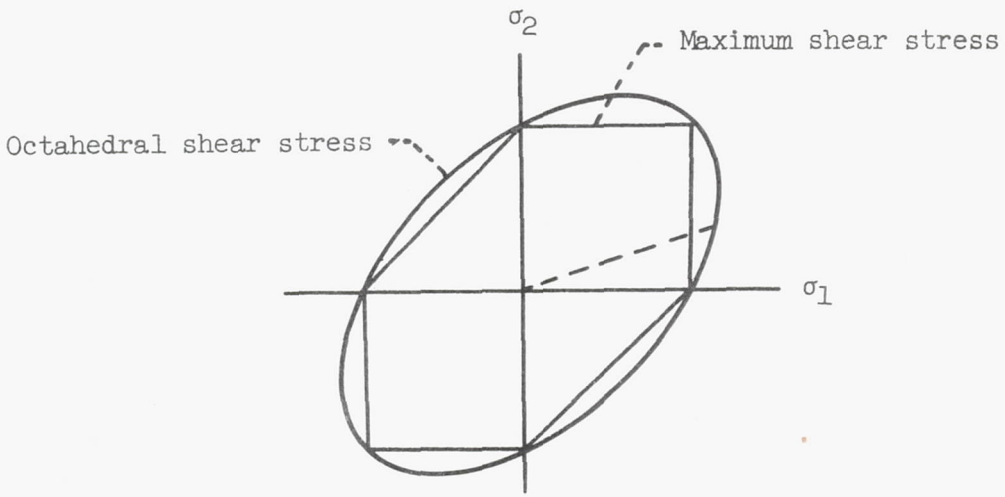

It is seen that the material near the midthickness of the test specimens where σ_2 is a maximum requires a higher value of σ_1 for plastic deformation, as indicated by the dashed line, than does material not subjected to this biaxial condition. In effect this means that the stress-strain curve for the material is raised above that for the standard tension specimens. As yet, only the influence of biaxiality on the plastic-deformation characteristics has been discussed.

The influence of biaxiality on the fracture characteristics of aluminum alloys must also be considered. In this respect the work of Dorn (ref. 5) is illuminating. He found that both 2024-T81 and 7075-T6 obeyed a maximum-shear-stress criterion of fracture.[1] If this be the case, the stress in the thickness direction which affects the plastic deformation of aluminum can have no influence on the fracture strength of the material. Then, since the maximum shear stress is a function of σ_1 and σ_3 only, and since σ_3 is zero, fracture is solely a function of σ_1 and biaxiality is without influence on the fracture stress.

Since the method of calculation described in reference 1 depends upon the shape of the stress-strain curve, these influences on flow and fracture must be taken into account when dealing with thick specimens in order to make predictions with reasonable accuracy. Figure 11 is a plot showing the modification for biaxiality in the flow stress curves which would bring about satisfactory agreement between theory and experiment for the 7075-T6 extrusion. Flow stress was increased when biaxiality was taken into account, but the fracture stress remained unchanged. A 40-percent reduction in the strain at maximum stress is required for the 7075-T6 extruded bar. This amounts to only a 1- to 2-percent rise in the plastic portion of the stress-strain curve. The magnitude of the change in elongation due to biaxial effects would be dependent upon the slope of the curve in the plastic range; the steeper the slope, the smaller the change. Therefore, the predictions for 2024-T4, which are seen to be slightly conservative without biaxial stress considerations (fig. 7), would be much less affected by such considerations, since the slope of the stress-strain curve in the plastic region is fairly steep. Figure 8 also includes the stress-strain curve for 2024-T4 as modified for biaxiality by raising the stress-strain curve 1 percent.

In figure 8 predictions of the modified theory that includes biaxiality are compared with the results of the experiments. It is seen that, in general, consideration of biaxiality greatly improves the agreement. Consideration of biaxiality lowers the predictions for 7075-T6. However, it is remarkable that the effect of biaxiality for 2024-T4 is to raise the predicted curve in the direction of the data points. This effect comes about because the net section stresses are above the proportional limit, and the factor E_u/E_n which determines the effect of plasticity on the theoretical stress concentration factor (ref. 1) decreases for this case, although E_u actually increases.

---

[1]In Dorn's work, the data were analyzed on the basis of true stresses and true strains, whereas in the present investigation engineering stresses and strains are used. The assumption is now made that the maximum-shear-stress law for fracture applies to engineering stresses as well as true stresses. This assumption seems reasonable since Dorn reported that "Under all biaxial stresses investigated, except for pure tension, the specimens fractured without evidence of necking. The neck developed in tension was small and was therefore neglected."

APPENDIX B

EFFECT OF DUCTILITY ON FRACTURE

The results of the present investigation indicate that the cross-grain static strength of fatigue-cracked 3/4- by 6-inch 7075-T6 extrusions is on a par with the with-grain static strength. However, this may not always be the case, and the results of the present investigation should not be generalized. The purpose of this appendix is to show, on the basis of a previously proposed theory (ref. 1), how the shape of the stress-strain curve can govern the notch sensitivity for static failure of a material.

In reference 1 it was shown that the stress concentration factor at static failure K_u for a fatigue crack is related to the elastic stress concentration factor modified for size effect K_N by the relation

$$K_u = 1 + \left(K_N - 1\right) \frac{E_u}{E_n} \tag{1}$$

where E_u is the secant modulus at maximum stress and E_n is the secant modulus corresponding to the stress on the net section at failure. For fatigue cracks in a material such as 7075-T6, the stress on the net section at failure is always below the proportional limit. As a consequence E_n is equal to Young's modulus. For such a case it is seen that, for a given value of K_N, K_u depends strongly on E_u.

In order to demonstrate how E_u can vary with direction in an actual case, the data of Templin, Howell, and Hartmann (ref. 2) for a $1\frac{1}{4}$- by $4\frac{1}{2}$-inch extrusion will be used. Stress-strain curves based on the material properties for a 7075-T6 extrusion are presented in figure 9 for both the with-grain and cross-grain directions. In contrast to the similarity for these directions exhibited by the 3/4- by 6-inch extrusion described in the body of this report, the stress-strain curves of the $1\frac{1}{4}$- by $4\frac{1}{2}$- inch extrusion are quite different in the two directions, with values of E_u which are in the ratio 2.29:0.84 or 2.72:1.

On the basis of these values, the calculated percentage of material tensile strength remaining was plotted against the percentage of the original area that was cracked (fig. 10). The specimen configuration was taken to be the same as that shown in figure 2. No correction for

biaxiality has been made, and for purposes of comparison it can be assumed that such effects are negligible, as in a thin sheet. It is apparent that the low ductility of the cross-grain material results in a considerable loss in static strength as compared with that predicted for the with-grain material. From these theoretical predictions it can be seen that an evaluation of the relative notch sensitivity might be obtained through a comparison of the stress-strain curves for the directions of interest.

The strong influence of ductility, as measured by the elongation at maximum load, on the notch sensitivity under static loading for the materials discussed in this report leads to a consideration of the amount of elongation required to obtain a level of notch sensitivity low enough to insure satisfactory performance in an aircraft structure. (At low precentages of elongation, the elongation at maximum stress and the percentage elongation over some usual gage length will be similar, since failure occurs close to maximum load with little necking.) An estimate of the necessary percentage elongation at maximum stress can be obtained by using the theory developed in reference 1. According to equation (1), notch sensitivity for sharp notches (i.e., notches that cause failure when the net section stress is below the proportional limit) is determined by the ratio E_u/E.

In order to illustrate the effect of elongation at maximum load on E_u/E for various aircraft structural materials, figure 12 has been prepared. The curves show the variation of E_u/E for specified values of tensile strength for these materials as a function of elongation at maximum stress. Note that in order to maintain a certain level of notch sensitivity (i.e., certain level of E_u/E) while increasing the strength of a given material, it is necessary that the elongation also increase. Unfortunately, materials generally show the reverse trend, and as a result the notch sensitivity increases with increase of tensile strength. Figure 12 also reveals that notch sensitivity for these materials increases rapidly for elongations of less than about 6 percent. For greater elongations the notch sensitivity is relatively independent of strain. In order to obtain a low level of notch sensitivity in the presence of sharp notches such as fatigue cracks, it appears, then, that the elongation at maximum stress should exceed 6 percent.

REFERENCES

1. McEvily, Arthur J., Jr., Illg, Walter, and Hardrath, Herbert F.: Static Strength of Aluminum-Alloy Specimens Containing Fatigue Cracks. NACA TN 3816, 1956.

2. Templin, R. L., Howell, F. M., and Hartmann, E. C.: Effect of Grain Direction on Fatigue Properties of Aluminum Alloys. Aluminum Co. of America, Reprinted From Product Engineering, July 1950.

3. Illg, Walter: Fatigue Tests on Notched and Unnotched Sheet Specimens of 2024-T3 and 7075-T6 Aluminum Alloys and of SAE 4130 Steel With Special Consideration of the Life Range From 2 to 10,000 Cycles. NACA TN 3866, 1956.

4. Taylor, G. I., and Quinney, H.: The Plastic Distortion of Metals. Phil. Trans. Roy. Soc. (London), ser. A, vol. 230, 1931, pp. 323-362.

5. Dorn, John E.: The Effect of Stress State on the Fracture Strength of Metals. Fracturing of Metals, A.S.M., c.1948, pp. 32-50.

TABLE I.- TENSILE PROPERTIES OF 7075-T6 ALUMINUM-ALLOY EXTRUDED BAR

[3/4-inch by 6-inch bar]

Direction	Yield stress (0.2% offset), ksi	Ultimate strength, ksi	Total elongation (2-inch gage length), percent	Young's modulus, ksi	Number of specimens
With-grain	77.9	89.0	13.3	10.6×10^3	12
Cross-grain	73.8	83.5	12.7	10.6×10^3	8

TABLE II.- RESULTS OF STATIC TESTS

Specimen	Grain direction	Crack profile	Percent of original area cracked	Static strength, ksi	Percent of material strength
1	Cross-grain		0	97.6	111.7
2	Cross-grain		.7	80.3	96.3
[a]3	Cross-grain		3.2	54.9	65.8
[b]4	Cross-grain		6.1	48.0	57.5
[a]5	Cross-grain		14.3	36.3	43.5
6	Cross-grain		15.2	36.3	43.5
[a]7	Cross-grain		17.9	36.3	43.5
[a]8	Cross-grain		28.0	27.6	33.0
9	Cross-grain		33.3	23.4	28.1
10	Cross-grain		37.4	15.1	18.1
11	Cross-grain		43.0	18.7	22.4
12	Cross-grain		45.4	20.1	24.1
13	Cross-grain		52.7	28.0	33.5
[a]14	Cross-grain		54.6	18.1	21.7
15	With-grain		9.3	67.0	75.3
16	With-grain		25.7	32.2	36.6
17	With-grain		54.6	10.7	12.0

[a]Fractured during cyclic loading.

[b]Crack initiated with sawcut.

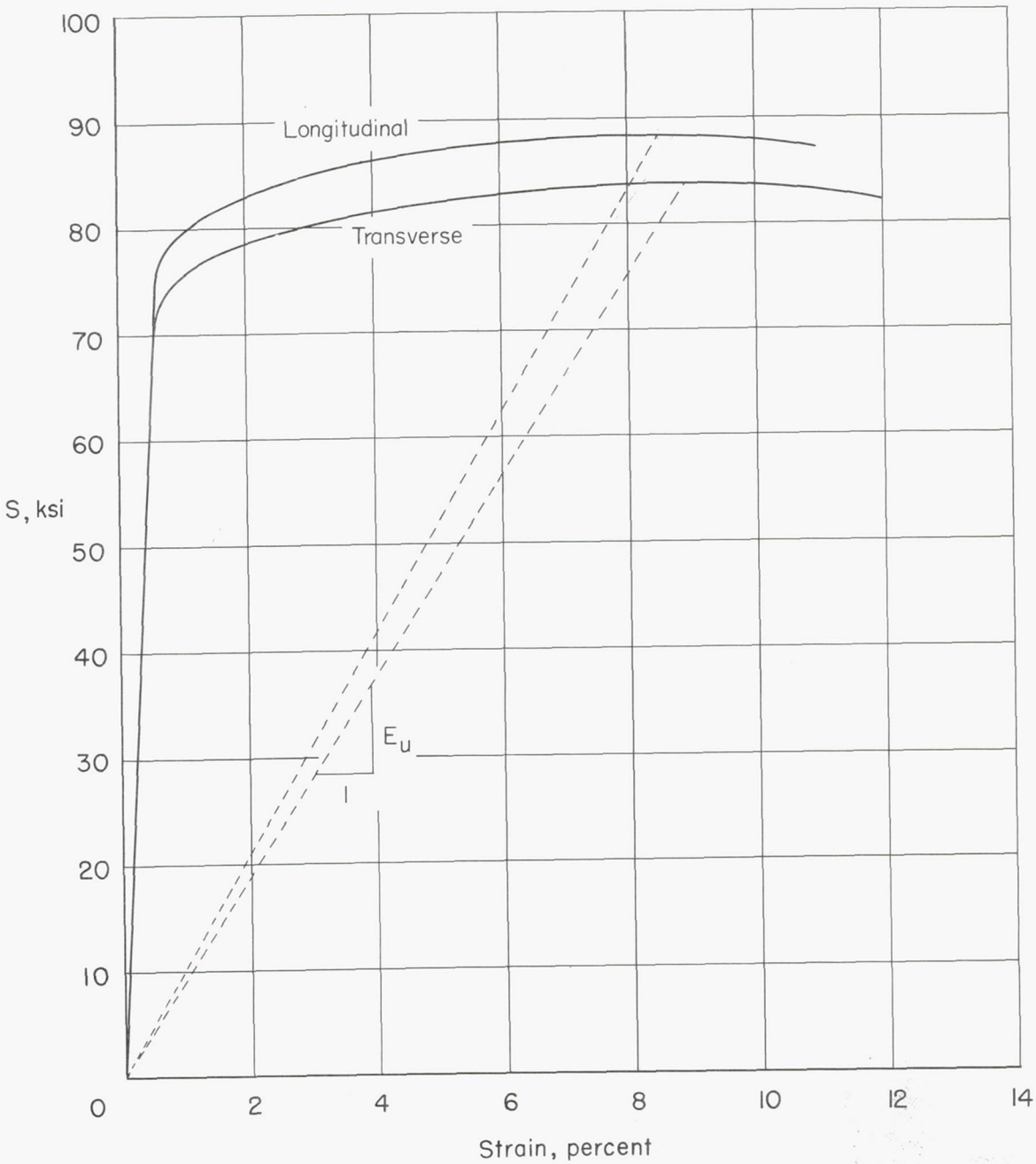

Figure 1.- With-grain and cross-grain stress-strain curves for 3/4- by 6-inch 7075-T6 extruded bar.

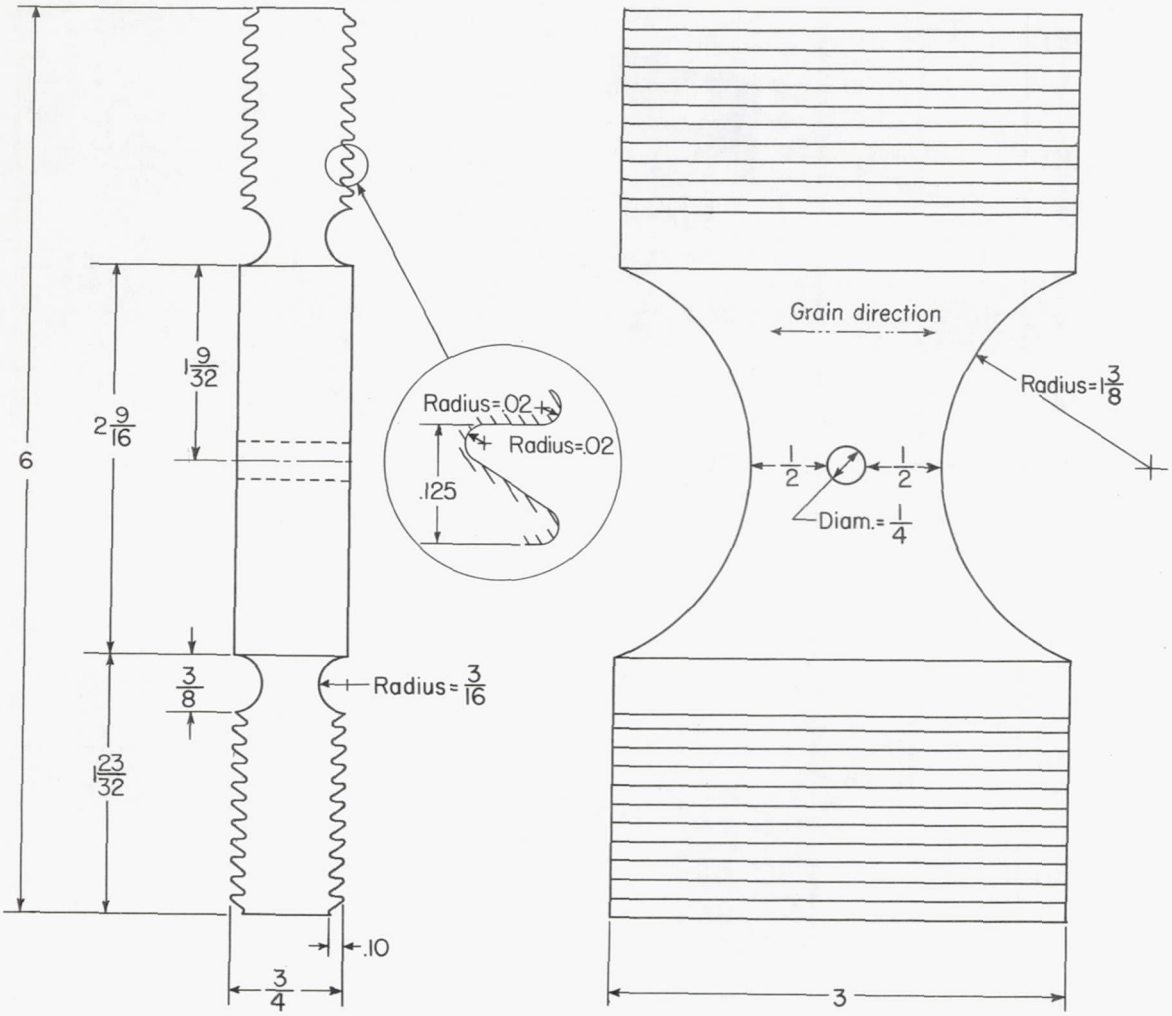

Figure 2.- Configuration of test specimens.

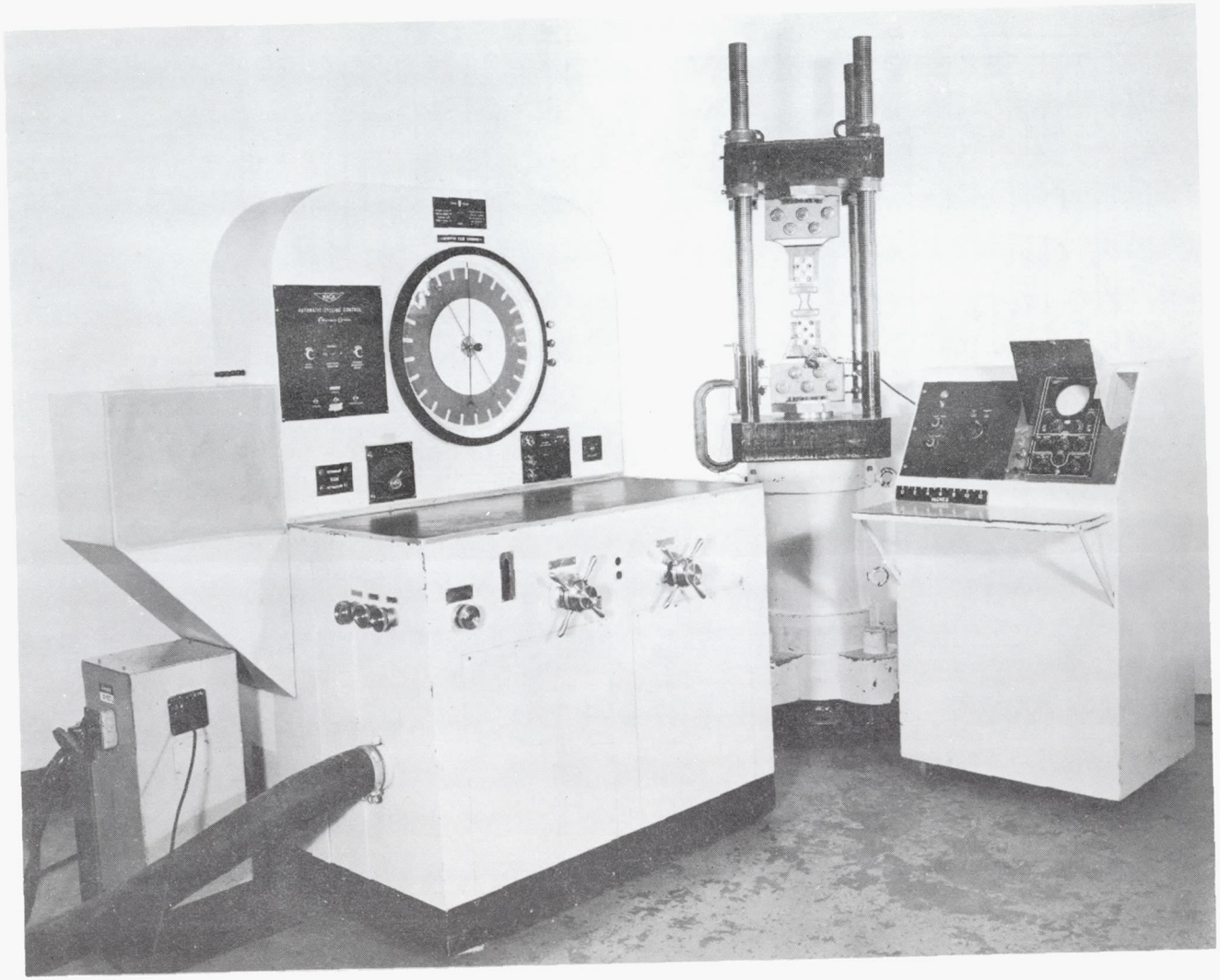

Figure 3.- Testing machine with specimen in place. L-93917.1

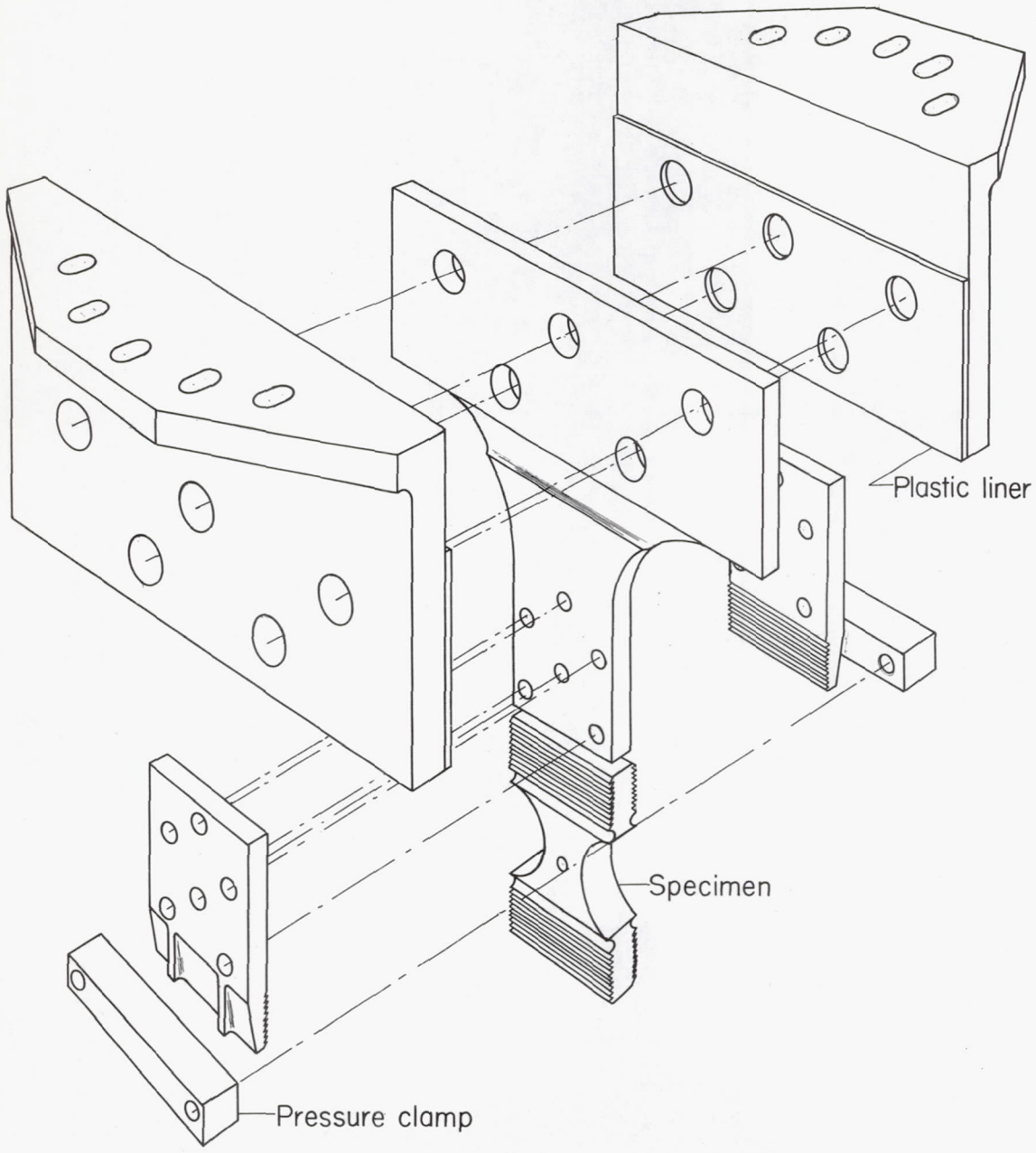

Figure 4.- Exploded view of grips and specimen. (Lower grips were identical to those shown.)

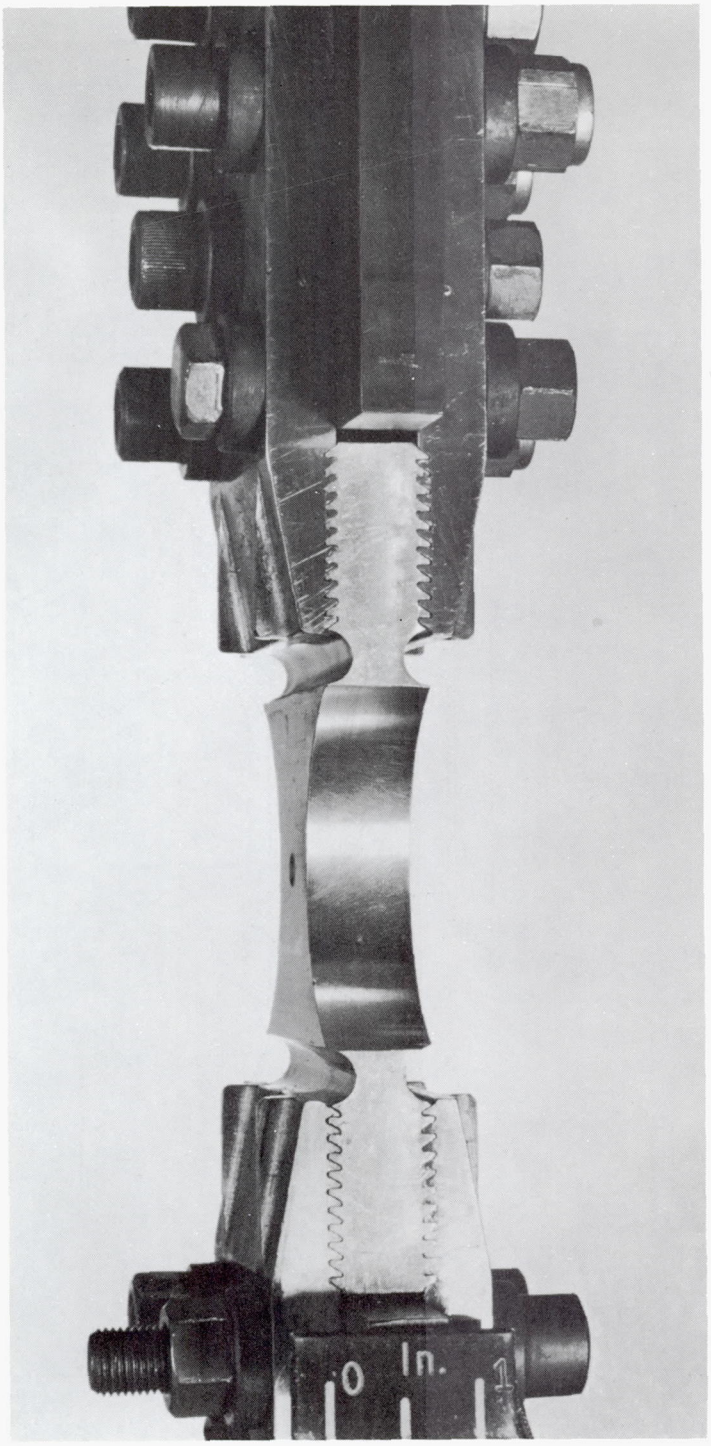

L-93919.1

Figure 5.- Closeup view of specimen in testing machine. (Pressure clamps are omitted for clarity.)

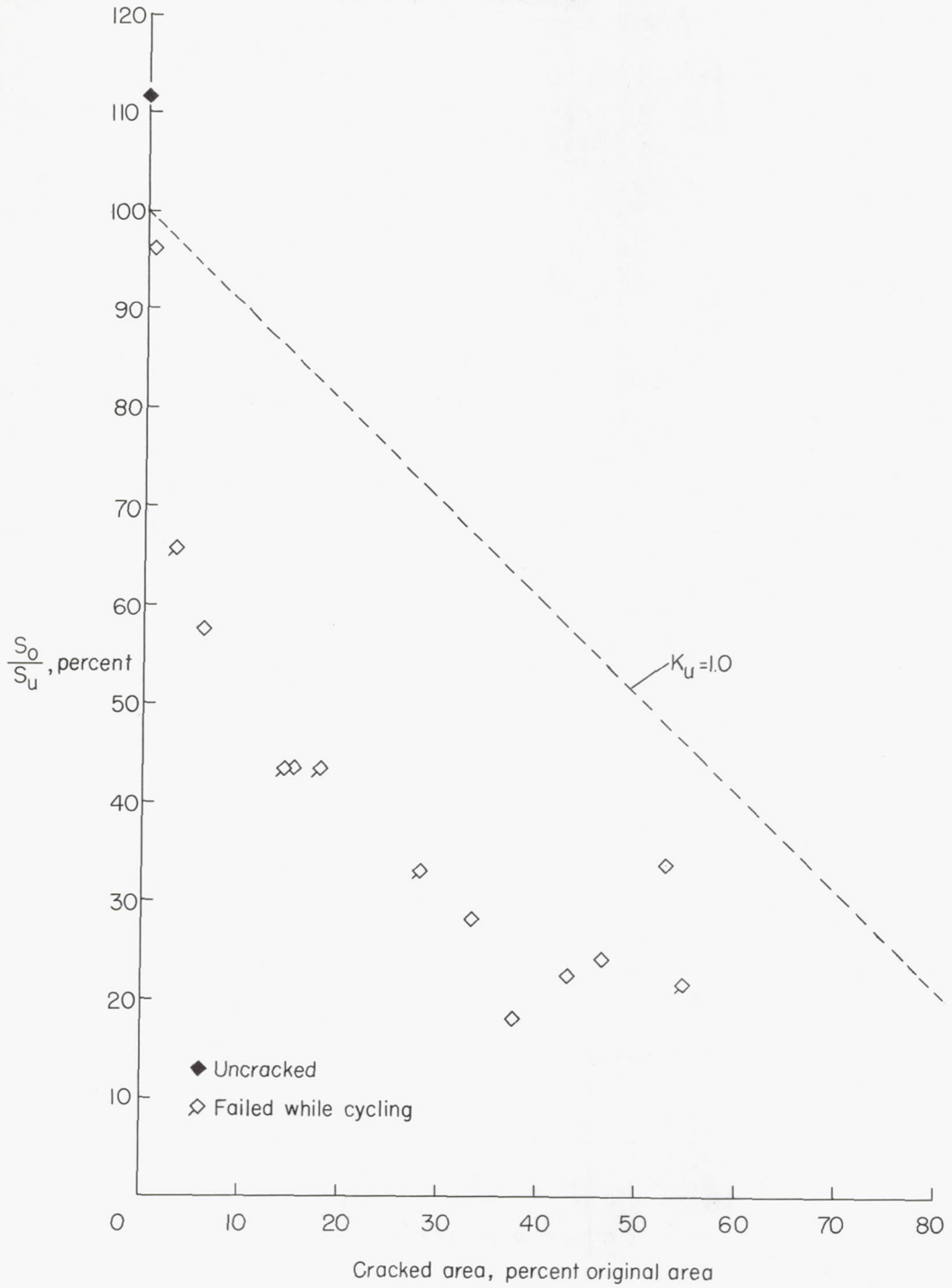

Figure 6.- Effect of fatigue cracks on strength of 3/4-inch-thick cross-grain 7075-T6 extruded bar.

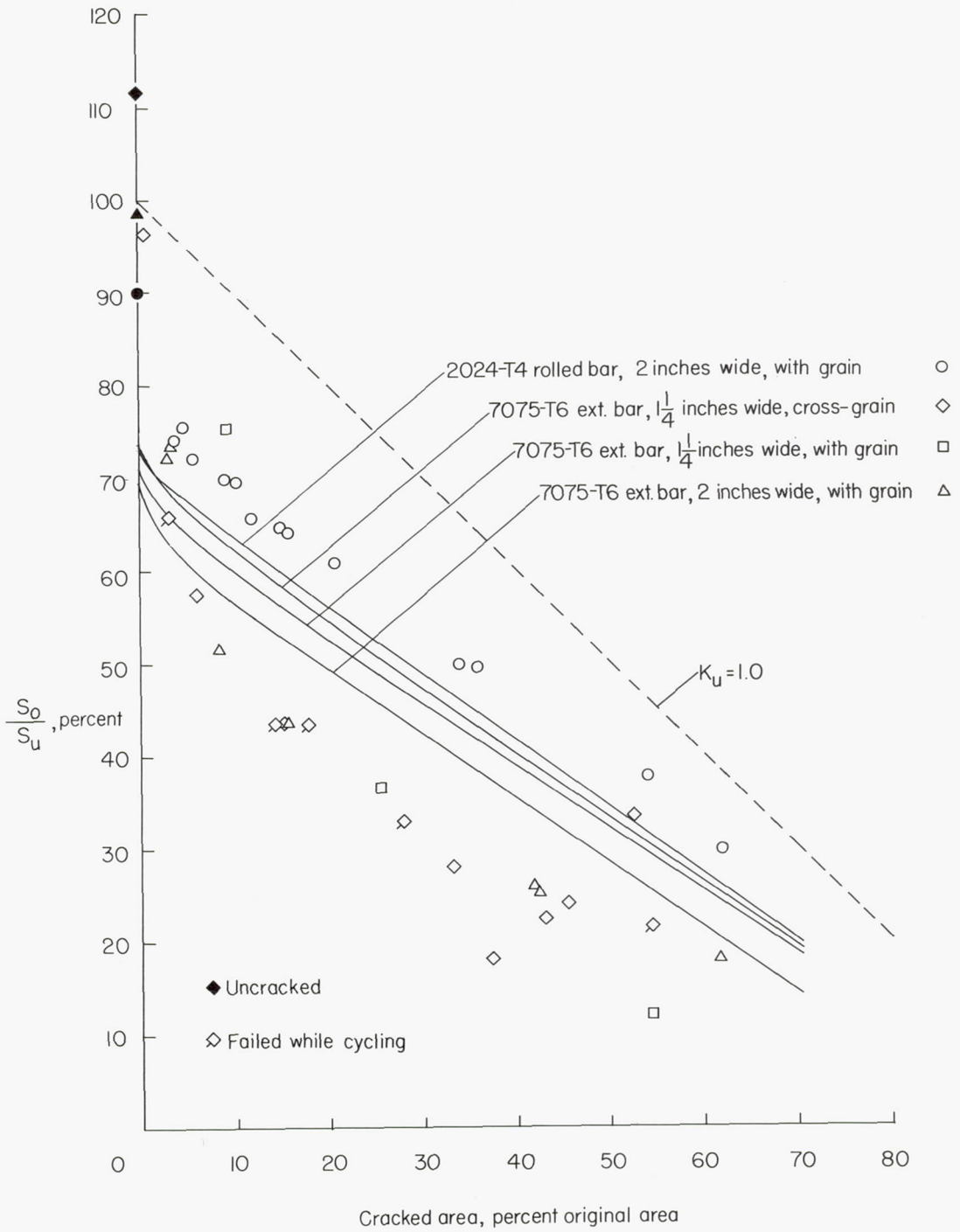

Figure 7.- Comparison of experimental results and theory for 7075-T6 extruded bar and 2024-T4 rolled bar, both 3/4-inch thick. (Symmetrical cracks were assumed in computing curves.)

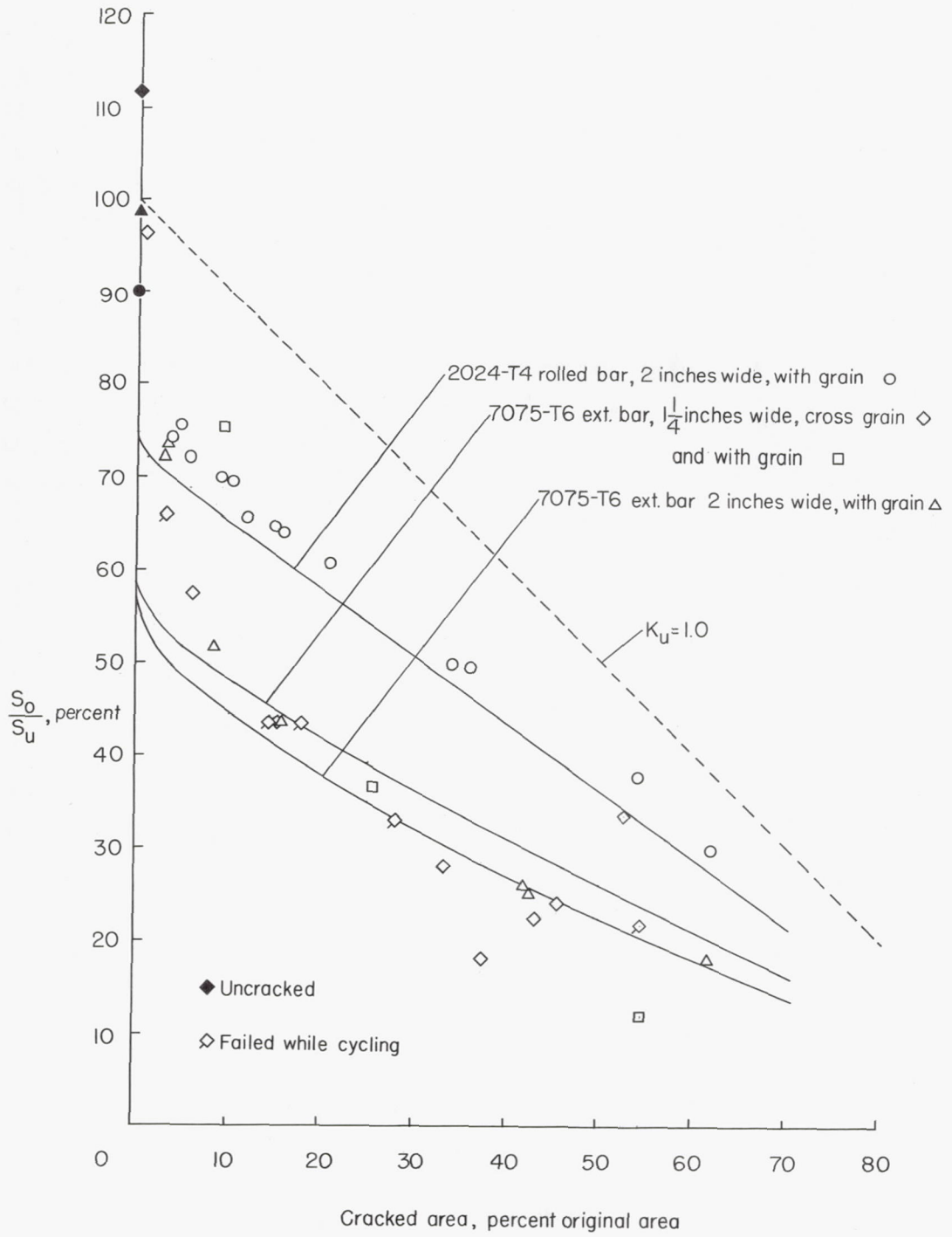

Figure 8.- Comparison of experimental results and theoretical predictions as modified by consideration of biaxiality. (Symmetrical cracks were assumed in computing curves.)

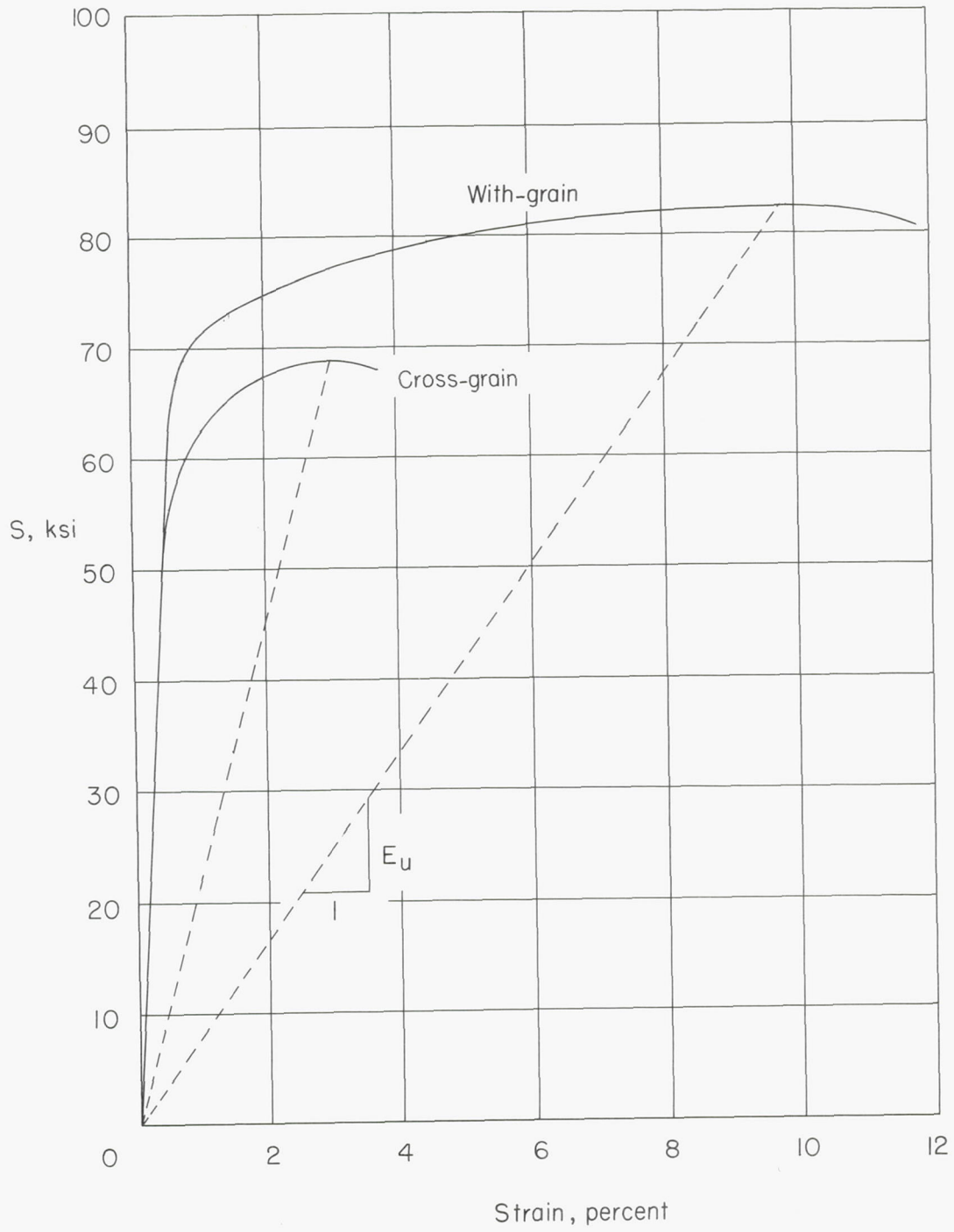

Figure 9.- With-grain and cross-grain synthesized stress-strain curves for a $1\frac{1}{4}$- by $4\frac{1}{2}$-inch 7075-T6 extruded bar.

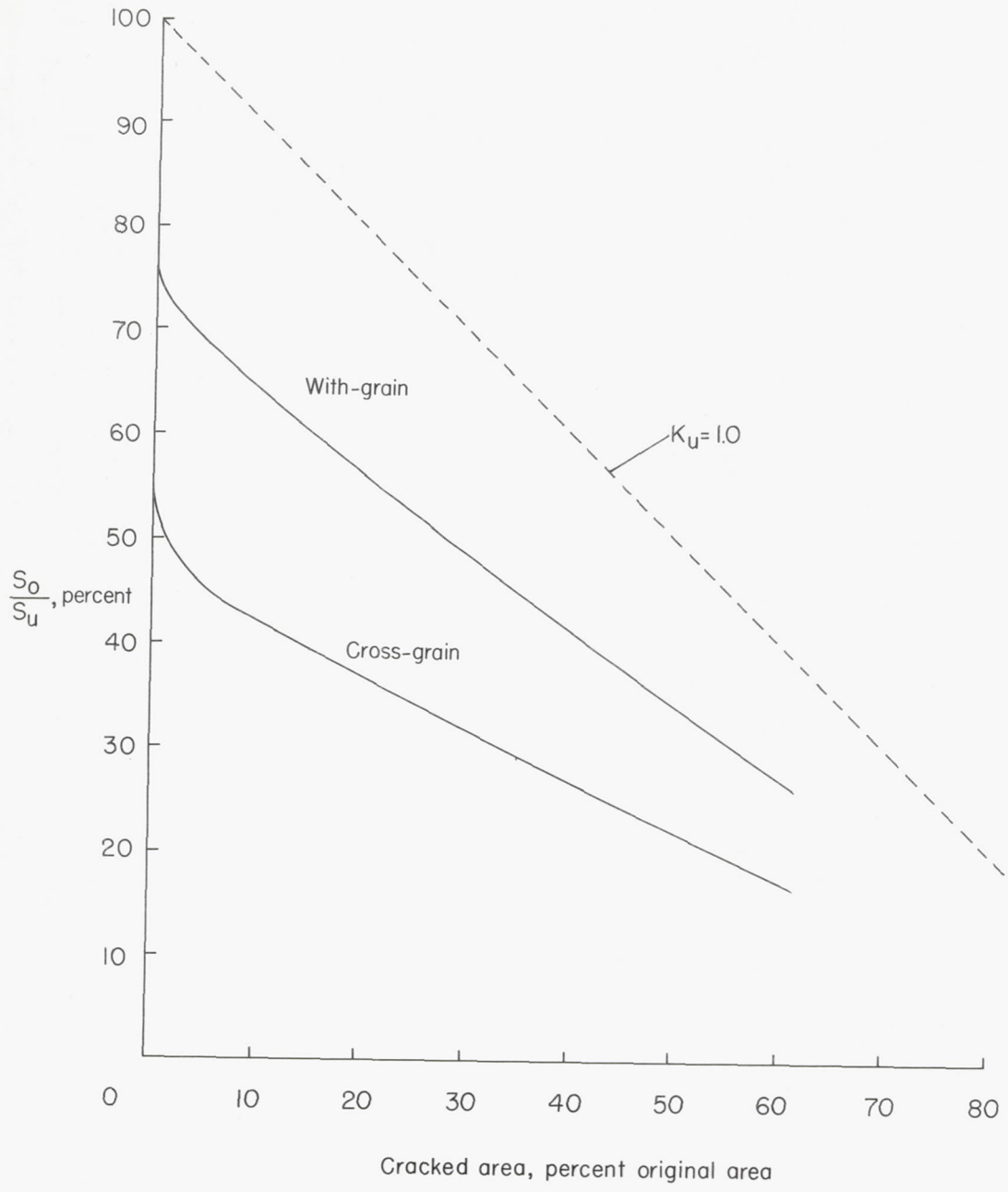

Figure 10.- Predicted effect of fatigue cracks on static strength of $1\frac{1}{4}$-inch-thick 7075-T6 extruded bar for both with-grain and cross-grain directions. (Symmetrical cracks were assumed in computing curves.)

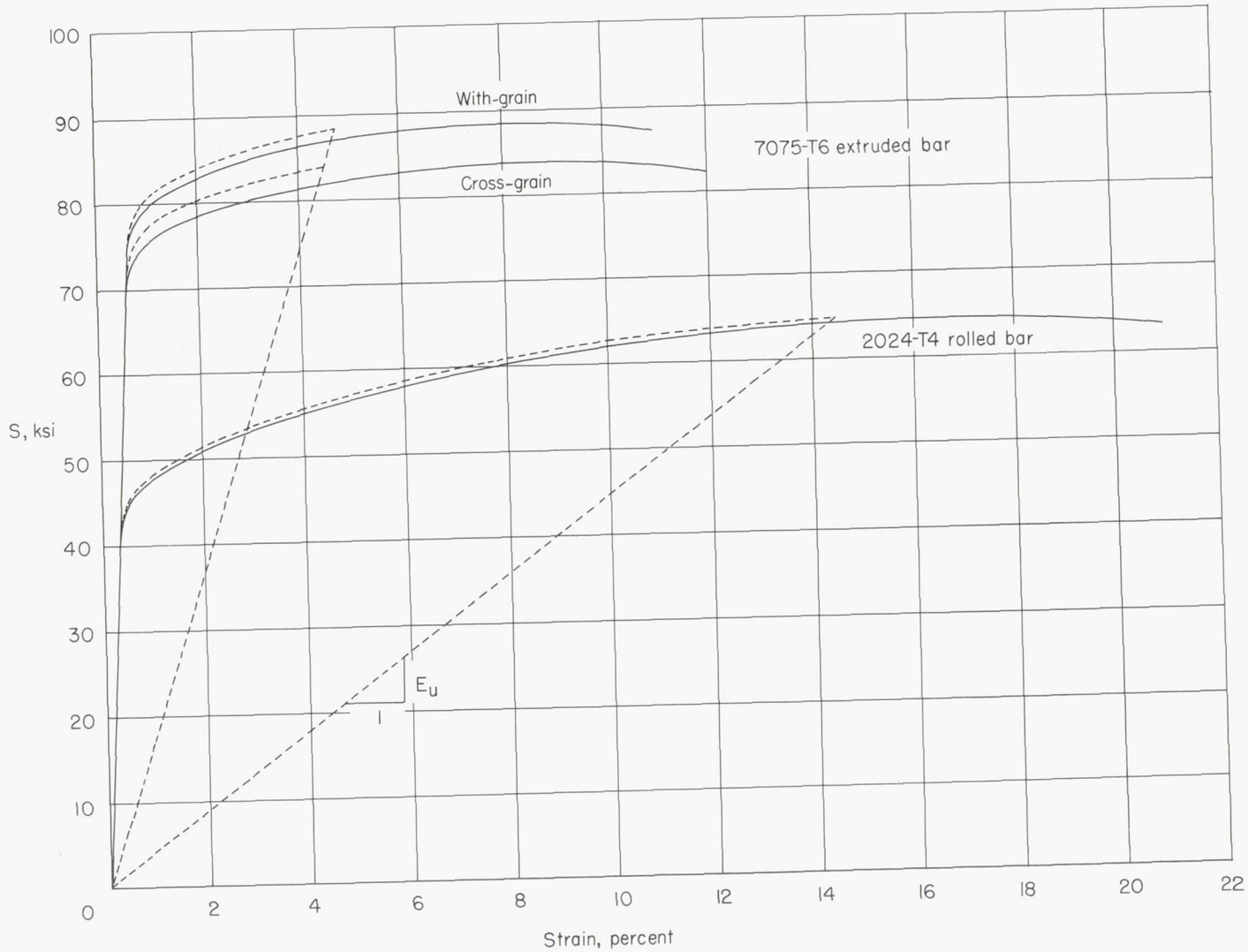

Figure 11.- Stress-strain curves modified for biaxiality (dashed curves) for 7075-T6 extruded bar and 2024-T4 rolled bar, both 3/4-inch thick.

Material	Young's modulus, ksi	S_{max}, ksi				
		1	2	3	4	5
Steel	30,000	300	200	150	100	50
Aluminum	10,000	100	67	50	33	17
Magnesium	6,400	64	48	32	24	12
Titanium	15,000	150	100	75	50	25

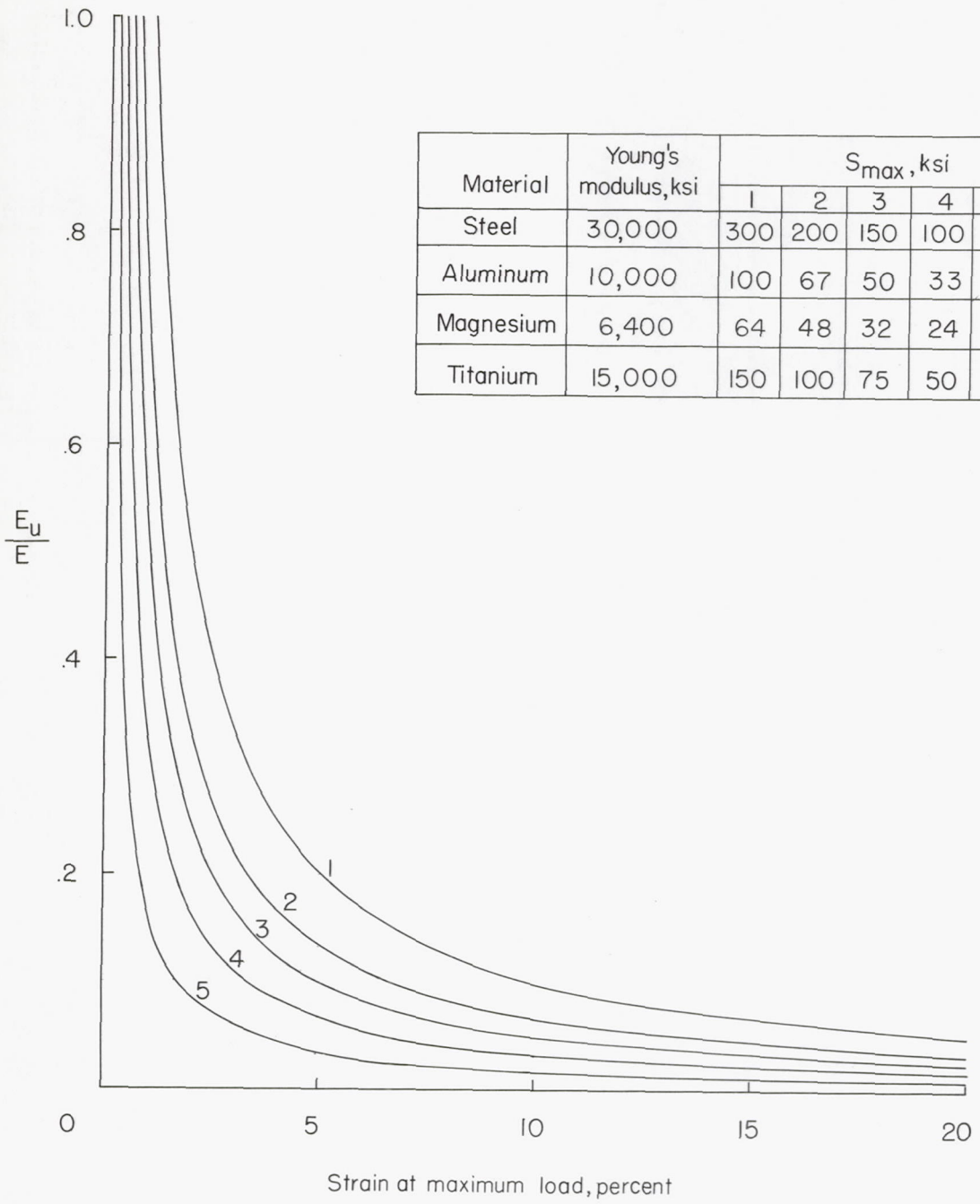

Figure 12.- Effect of notch-sensitivity index E_u/E on percent elongation at maximum load.